Slot-Array Antennas Fed by Coplanar Waveguide for Millimeter-Wave Radiation

Hiroaki Kobayashi and Yoshizumi Yasuoka

***Abstract*— Slot-array antennas with parasitic slots, slot-array antennas fed by coplanar waveguide (CPW), and two-dimensional slot-array antennas fed by CPW were fabricated on fused quartz substrates, and the receiving properties of the antennas were investigated at 94 GHz with the goal of increasing the power gain of the slot antennas. It was found that the power gain of the slot antenna could be increased by 11 dB over a single-slot antenna by using a two-dimensional (8 $\times$ 3) slot-array antenna fed by CPW. It was confirmed that the improvement of the power gain was caused by decreasing surface-wave power in the substrate and by sharpening antenna patterns perpendicular to the substrate.**

***Index Terms*—Array antenna, coplanar waveguide, millimeter wave, slot antenna, submillimeter wave, thin-film antenna.**

I. Introduction

THE demand for millimeter- and submillimeter-wave systems consisting of planar antennas has recently increased in communication systems, remote sensing, radio astronomy, and plasma diagnostics. Some planar array antennas fed by a waveguide structure for millimeter-wave radiation have been reported [1]–[3]. However, the waveguide structure is too complex to fabricate in the submillimeter-wave region. On the other hand, a thin-film antenna placed on the dielectric substrate is relatively easy to fabricate through recently developed microfabrication techniques. These techniques have encouraged the fabrication of thin-film antennas, transmission lines, and detectors on the coplanar substrate. Also, new research has been done on thin-film devices for millimeter- and submillimeter-wave radiation [4]–[6].

As thin-film antennas for millimeter- and submillimeter-wave systems, the dipole [7], slot [8], [9], microstrip [10], spiral [11], and log periodic [12] antennas have been studied. In these antennas, the slot antenna had a simple structure and directivity perpendicular to the substrate. These characteristics make the slot antenna suitable for array antennas in the millimeter- and submillimeter-wave regions. The authors previously studied the single-slot antennas for millimeter- and submillimeter-wave radiation [13], [14], and confirmed that the single-slot antenna on the thick dielectric substrate lost 72% of the radiated power due to the surface-wave modes trapped in the substrate when fused quartz (dielectric constant $\varepsilon_r = 3.8$) was used as the substrate [15]. The power lost to the surface-wave modes was decreased to 36% by using the four slot-array antenna with two parasitic slots, and the power gain was improved by 5 dB over the single-slot antenna at 94 and 700 GHz [16], [17]. However, it is considered that the coupling efficiency between two parasitic slots could still be improved, and that it would be effective to couple the slots with coplanar waveguide (CPW) in order to achieve the improvement of the power gain.

In this paper, slot-array antennas with parasitic slots, slot-array antennas fed by CPW, and two-dimensional slot-array antennas fed by CPW were fabricated on a fused quartz substrate, and the antenna pattern and power gain of the three types of antennas were compared and discussed at 94 GHz.

II. Configuration of the Slot-Array Antennas

Fig. 1 shows the configuration of the proposed slot-array antennas. Fig. 1(a) is the configuration of the slot-array antenna with parasitic slots [18]. The antenna consists of the two resonant slots fed by CPW and parasitic slots. The dimensions of the slot antenna have been determined on the basis of the experimental results obtained at the microwave frequency. The length and width of the slots are 0.72 and 0.08 λ_m, respectively [13], where λ_m is the mean wavelength [19]. The separation of two slots d_k is $(k - 0.4)\lambda_d$, as shown in the Fig. 1(a), where λ_d is the dielectric wavelength. The separation were theoretically determined as the one where the surface-wave power (TM wave) in the substrate becomes the smallest [18]. This has been confirmed by experiments [16]. The antennas were fabricated on a fused quartz substrate ($\varepsilon_r = 3.8$) with thicknesses in odd multiples of a quarter dielectric wavelength ($h = 2.25\ \lambda_d$) with a photolithographic method [16]. According to the previous paper, the power gain of the antenna fabricated on the dielectric substrate changes periodically with the thickness of the substrate. The gain of the antenna on the substrate with the thickness in odd multiples of a quarter dielectric wavelength is higher by 6 dB than the one with the thickness in even multiples [15]. A bismuth microbolometer is used as the detector [20], and is placed at the center of the CPW.

Fig. 1(b) shows the configuration of the slot-array antenna fed by CPW. The length of CPW between each pair of slots was made to be 1 λ_m in order that all the slots would be excited with an equal phase. The shape of winding CPW is called the "meander line" in this paper. The other dimensions and separations of the slots were identical with the antenna shown in Fig. 1(a). The width of the conductor s and the

Manuscript received October 15, 1997; revised March 4, 1998.

The authors are with the Department of Electronic Engineering, National Defense Academy, Yokosuka 239-8686, Japan (e-mail: yasuoka@cc.nda.ac.jp).

Publisher Item Identifier S 0018-9480(98)04043-5.

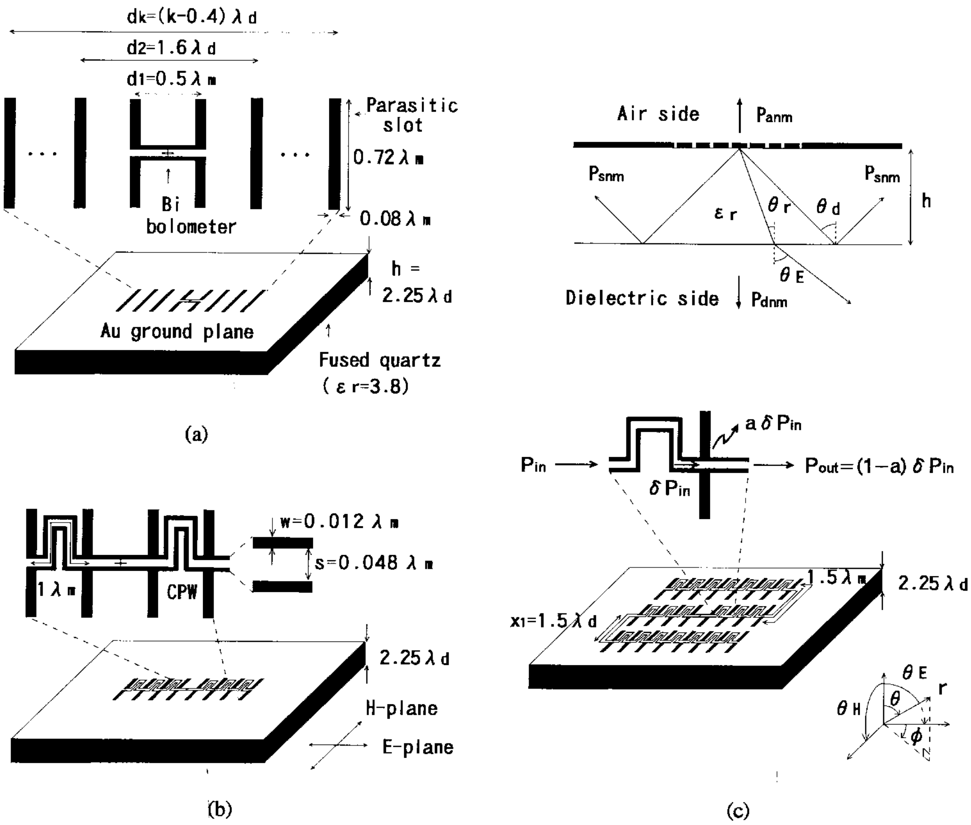

Fig. 1. Configuration of the proposed slot-array antennas. (a) Slot-array antenna with parasitic slots. (b) Slot-array antenna fed by CPW. (c) Two-dimensional slot-array antenna fed by CPW.

spacing of the conductor w of the CPW are 0.048 and 0.012 λ_m, respectively. The total width of CPW $s+2w$ is determined thinner than one-tenth of the antenna length in order to maintain the resonant frequency [13].

Fig. 1(c) shows a two-dimensional slot-array antenna fed by CPW. The E-plane array is the same as shown in Fig. 1(b). The separation between each pair of lines in the H-plane was determined to be 1.5 λ_d in order to decrease surface-wave power (TE wave) in the substrate [18]. The length of CPW between each pair of lines was 1.5 λ_m in order that all the slots could be excited with an equal phase.

III. Theory

The analysis of an infinitesimal slot antenna carried out by Rutledge *et al.* [21] was extended to a one-wavelength resonant slot antenna, so that the effects of substrate thickness on the power gain of the single-slot antenna could be studied theoretically and experimentally [15]. Also, the analysis of the single-slot antenna was extended to more than two slot-array antennas, and the receiving properties of slot-array antennas with parasitic slots on the dielectric substrates were studied theoretically and experimentally [18]. In this paper, the analysis of the two-dimensional slot-array antennas fed by CPW is introduced by supplementing the analysis of the slot-array antennas with the transmission properties of CPW.

The theoretical E-plane pattern $G_m(\theta_E)$ and the H-plane pattern $G_m(\theta_H)$ of the $n \times m$ (E-plane $\times H$-plane) slot-array antenna on the dielectric substrate side can be calculated using a transmission-line model given by the following equations [18]:

$$G_m(\theta_E) = 2G_{nm}\frac{P_{\rm anm}}{P_0} \cdot \frac{D_n(\theta_E)}{\cos^2\varphi + \left[\cos\theta_r/\left(\sqrt{\varepsilon_r}\cos\theta_E\right)\right]^2 \sin^2\varphi} \tag{1}$$

$$G_m(\theta_H) = 2G_{nm}\frac{P_{\rm anm}}{P_0} \cdot \frac{D_m(\theta_H)}{\cos^2\varphi + \left[\cos\theta_H/\left(\sqrt{\varepsilon_r}\cos\theta_r\right)\right]^2 \sin^2\varphi} \tag{2}$$

$$\varphi = 2\pi\frac{h}{\lambda_d}\cos\theta_r. \tag{3}$$

G_{nm} is the directive gain of $n \times m$ slot-array antenna in the free space. $P_{\rm anm}/P_0$ is the ratio of radiating power of $n \times m$ slot-array antenna on the air side to the total power radiated by the single-slot antenna in the free space P_0. $D_m(\theta_E)$ and $D_m(\theta_H)$ are the normalized E-plane pattern and the H-plane pattern of $n \times m$ slot-array antenna on the air side, respectively. θ_r is the refractive angle and φ is the electrical thickness of the substrate.

When each slot placed at the separation of $d_1, d_2, \cdots, d_k$ in the E-plane excites in equal phase, the E-plane pattern

$D_m(\theta_E)$ is given as follows [22]:

$$D_n(\theta_E) = C_1 \left\{ \cos(\pi d_1 \sin\theta_E/\lambda_0) + \sum_{k-1}^{n/2-1} \left[\sqrt{A_{k+1}} \cos(\pi d_{k+1} \sin\theta_E/\lambda_0) \right] \right\}^2 \tag{4}$$

where $1, A_2, \cdots, A_k$ are power coefficient radiated from each slot, and C_1 is a normalized coefficient. Also, when each slot placed at the separation of $x_1, x_2, \cdots, x_k$ in the H-plane excites in equal phase, the H-plane pattern $D_m(\theta_H)$ is given as follows [22]:

$$D_m(\theta_H) = C_2 D_1(\theta_H) \cdot \left\{ 1 + \sum_{k-1}^{(m-1)/2} \left[\sqrt{2B_k} \cos(2\pi x_k \sin\theta_H/\lambda_0) \right] \right\}^2 \tag{5}$$

where B_k is the power coefficient radiated from each slot #k, and C_2 is a normalized coefficient.

Hence, if the power coefficients A_k and B_k radiated from each slot are derived, the antenna patterns in (4) and (5) could be calculated. In Fig. 1(c), the transmitted power P_{out} is expressed $P_{\text{out}} = (1-a)\delta P_{\text{in}}$ by using the input power P_{in}, the transmission efficiency of CPW per λ_m δ, and the rate of the radiated power from the slot antenna a. The power radiated from each slot-array antenna n is given by the equation

$$P_{n/2} = \{(1-a)\delta\}^{n/2-1}. \tag{6}$$

The power coefficients A_k and B_k in (4) and (5) can be derived from (6) in the E- and H-planes, respectively.

The directive gain of $n \times m$ slot-array antenna in the free-space G_{nm} can be calculated by using (4) and (5), and is given as follows [23]:

$$G_{nm} = G_1 \left[\frac{4\pi}{\int_{-n}^{n} \int_{-n/2}^{n/2} D_n(\theta_E) \cos\theta d\theta d\phi} \right] \cdot \left[\frac{4\pi}{\int_{-n}^{n} \int_{-n/2}^{n/2} D_m(\theta_H) \cos\theta d\theta d\phi} \right] \tag{7}$$

where G_1 indicates the power gain of the single-slot antenna in free space and $G_1 = 2.8$ dBi in the case of the dimension shown in Fig. 1(a) [23].

In Fig. 1(c), P_{anm} shows the power radiated directly to the air from slots, P_{dnm} is the power radiated to the air through the dielectric substrate, and P_{snm} is the power coupled to the surface-wave mode in the substrate. Since the total power radiated from the slots is constant and independent of n, m, and h, and is equal to the total power radiated from the single-slot antenna in the free space P_0, then the following is true:

$$P_{\text{anm}} + P_{\text{dnm}} + P_{\text{snm}} = P_0. \tag{8}$$

P_{dnm}/P_0 is given by substituting (4) and (5) into [18, eq. (A.5)]. On the other hand, P_{snm}/P_0 is given by extending [18, eq. (A.6)] to the two-dimensional array antenna. P_{anm}/P_0 is given by substituting P_{dnm}/P_0 and P_{snm}/P_0 into (8). If the rate P_{anm}/P_0 is derived, the power gain $(\theta_{E,H} = 0)$ could be calculated from (1) and (2).

In this paper, the improvement of the power gain in (1) and (2) is caused by decreasing surface-wave power P_{snm}/P_0 and by increasing the directive gain G_{nm} in (7). The antenna patterns and power gains are obtained from the equations described above.

IV. Transmission Properties of the Coplanar Waveguide

The transmission efficiency of CPW per λ_m δ, and the rate of the radiated power from the slot antenna a are predicted on the basis of the experimental results obtained at the frequency of 2.2 GHz. The CPW is fabricated on a glass–fiber–reinforced plastic (FRP) substrate $(\varepsilon_r = 4.3)$ of 335 mm × 335 mm × 40 mm. The FRP substrate is used since the relative dielectric constant is close to that of the fused quartz substrate which will be used at the frequency of 94 GHz. The width of the conductor s and the spacing of the conductor w of the CPW are 4 and 1 mm, respectively [see Fig. 1(b)]. In the experiments, the δ was obtained by measuring the insertion loss S_{21} using the network analyzer at 2.2 GHz.

Fig. 2 shows relationship between the δ measured at 2.2 GHz and the number of meander lines. The symbol "●" shows the experimental results. The meander line is fabricated on the basis of the given values in Fig. 1(b). The measured δ of the straight CPW shows $0.85/\lambda_m$ [$n = 0$ in Fig. 2]. It is estimated from this value and [21] that the dielectric radiation loss is $0.1\text{dB}/\lambda_m$, and metal and dielectric absorption losses are $0.6\text{dB}/\lambda_m$. On the other hand, when $n \geqq 1$, the measured δ shows about $0.83/\lambda_m$. This value is slightly lower than that of straight CPW, and independent of the number of the meander line. It is believed that the small losses are caused at corners of the meander line. It was confirmed from the experiment that the transmission efficiency of the meander line became almost the same as that of the straight CPW when the right-angle corner was bent. These results indicate that the meander lines have very small losses and are useful for the slot-array antennas.

Fig. 3 shows the relationship between the normalized radiation power $a\delta P_{\text{in}}$ from the nth slot and the number of slots. The experiment was carried out at 2.2 GHz. The power radiated from each slot through the CPW was predicted by measuring the difference between S_{21} without slot and $S_{21'}$ with slot, as shown by the insertion figure in Fig. 3. The experimental data are shown by the symbol "●." Each line shows the theoretical values calculated by substituting $a = 0.4$, 0.5, 0.6 into (6) at $\delta = 0.83/\lambda_m$, respectively. The measured data agree well with the theoretical value at $a = 0.5$. These experimental data indicate that each slot radiates 50% of the

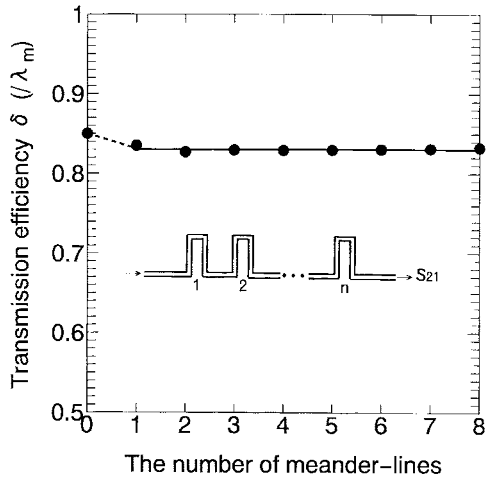

Fig. 2. Relationship between the transmission efficiency δ measured at 2.2 GHz and the number of meander lines.

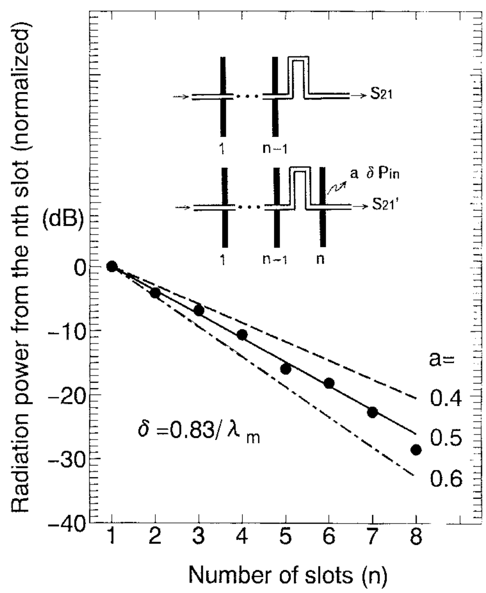

Fig. 3. Relationship between the normalized radiation power $a\delta P_{\rm in}$ from the nth slot and the number of slots at 2.2 GHz.

input power and the CPW transmits 50% of the remaining power to the next slot.

It was concluded that the transmission efficiency of the meander line and the rate of radiation power from the slot antenna obtained from the microwave model experiments are $\delta = 0.83/\lambda_m$ and $a = 0.5$, respectively. Therefore, these values were utilized for the experiments in the 94-GHz millimeter-wave region.

V. Receiving Properties of the Array Antennas at 94 GHz

Figs. 4–6 show the antenna patterns when the 94-GHz millimeter-wave signal was irradiated to the antenna through the substrates. Fig. 4 shows the antenna patterns of the single, two-, four-, six-, and eight-slot-array antennas with parasitic slots referred to [18]. In regard to the E-plane on the left side of the figure, the directivity became sharper as the number of slots was increased up to six. However, the antenna pattern did not become sharper with the increase of slots from six to eight. On the other hand, the antenna pattern did not change at all in the H-plane on the right side of the figure with an increased number of slots.

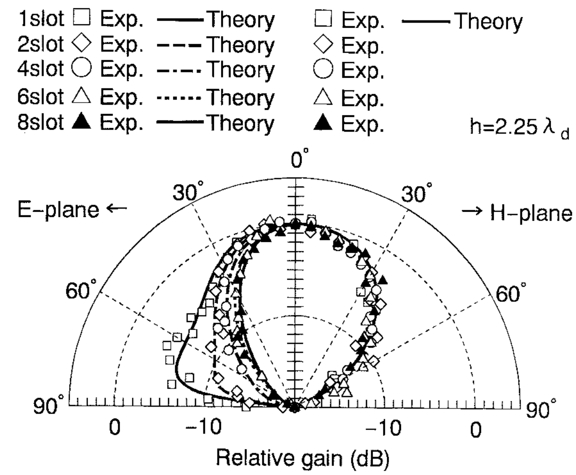

Fig. 4. Antenna patterns of the slot-array antenna with parasitic slots [see Fig. 1(a)] measured from the dielectric side at 94 GHz.

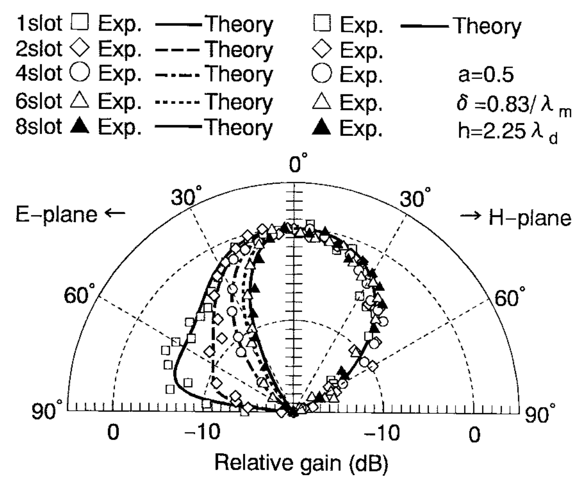

Fig. 5. Antenna patterns of the slot-array antenna fed by CPW [see Fig. 1(b)] measured from the dielectric side at 94 GHz.

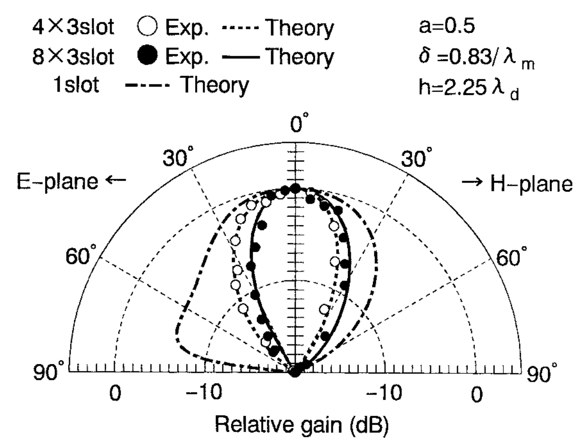

Fig. 6. Antenna patterns of the two-dimensional slot-array antenna fed by CPW [see Fig. 1(c)] measured from the dielectric side at 94 GHz.

Fig. 5 shows the antenna patterns of the single-, two-, four-, six-, and eight-slot-array antennas fed by CPW. In regard to the E-plane, the directivity became sharper as the number of slots

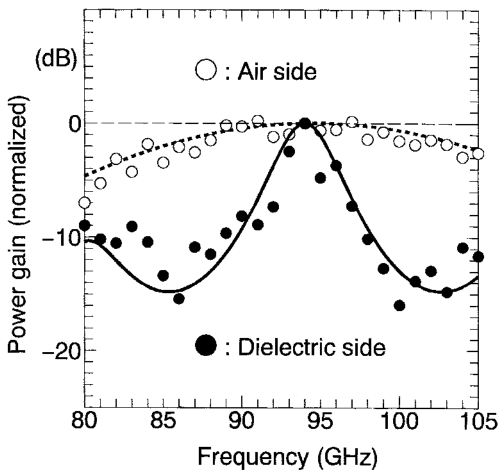

Fig. 7. Normalized power gain of the 4 × 3 slot-array antenna fed by CPW as a function of the frequency.

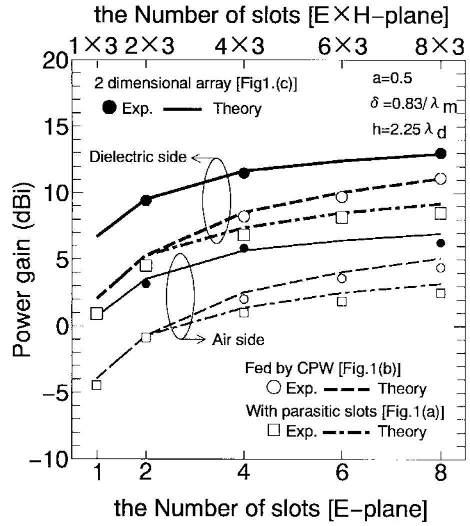

Fig. 8. Relationship between the power gain measured from the dielectric side at 94 GHz and the number of slots.

was increased up to eight, which agrees with the theoretical pattern when the δ and the a are assumed to be $0.83/\lambda_m$ and 0.5, as shown in Figs. 2 and 3, respectively. On the other hand, the antenna pattern did not change at all in the H-plane on the right side of the figure with an increased number of slots.

Fig. 6 shows the antenna patterns of the two-dimensional 4 × 3 and 8 × 3 (E-plane $\times H$-plane) slot-array antennas fed by CPW as well as the theoretical antenna patterns calculated using $\delta = 0.83/\lambda_m$ and $a = 0.5$. The figure also shows the theoretical patterns of the single-slot antenna. In the case of the two-dimensional 4 × 3 and 8 × 3 slot-array antennas, the directivities became sharper than that of the single-slot antenna. These finding are different from what is shown in Figs. 4 and 5. While the E-plane pattern of 8 × 3 array became sharper than the one of 4 × 3 array, the H-plane pattern of 8 × 3 array became duller than the one of 4 × 3 array. These results indicate that the directivity of the two-dimensional array antenna strongly depends on the power radiated from each slot, which are determined by the δ and the a.

Fig. 7 shows the normalized power gain of the 4 × 3 slot-array antenna fed by CPW as a function of the frequency. In the figure, the symbol "○" is the power gain of the antenna when the millimeter-wave signal was irradiated on the antenna directly from the air side, and the symbol "●" represents the power gain when the signal was irradiated to the antenna through the substrates. Here, both gain are normalized to 0 dB at 94 GHz, although the measured values of gain shown by the symbol "●" are higher by 6 dB than the ones shown by the symbol "○" at 94 GHz, as shown in Fig. 8. For the irradiated signal from the air side, the antenna has a center frequency at 94 GHz as theoretically predicted and has a 3-dB bandwidth of about 25%. This value is comparable to the theoretical bandwidth of the single-slot antenna [19]. For the signal irradiated through the substrate, the gain strongly depends on the substrate thickness [15]. Besides, the thickness of the substrate used in the experiment is 2.25 λ_d (odd multiples of the $\lambda_d/4$) at 94 GHz, and is 2.0 λ_d (even multiples of the $\lambda_d/4$) at 84 GHz and 2.5 λ_d (even multiples of the $\lambda_d/4$) at 104 GHz, respectively. In Fig. 7, the product of the substrate-thickness dependence (converted into frequency) of the power gain and the frequency dependence of the power gain obtained by the antenna (shown by the dotted curve in the figure) is shown by the solid curve for comparison.

Fig. 8 shows the relationship between the power gain and the number of slots in the three kinds of antennas, as shown in Fig. 1, when the 94-GHz signal was irradiated through the substrate. The symbols "●," "○," and "□" represent the measured power gain of the antennas, while each curved line represents the theoretical power gain obtained from (1) and (2). In the calculation of the power gain, the δ and the a are assumed to be $0.83/\lambda_m$ and 0.5, respectively, from Figs. 2 and 3.

The power gain of the slot-array antennas with parasitic slots increased with the increase of the number of slots up to six slots [18]. However, since the surface wave (TM wave) from the resonant slot fed by CPW spreads out in the substrate [21], the surface wave reached the arrayed parasitic slots rapidly decreases with the increase of the distance between the resonant slot and parasitic ones. The increase of the power gain with the increase of the number of slots then becomes quickly insignificant. This properties is predicted from the antenna patterns, as shown in Fig. 4.

In the case of the slot-array antennas fed by CPW, the surface wave from the resonant slot reaches the arrayed slots through the CPW. Then, the power gain still increases with the increased number of the slots from six to eight, which is different from the case of the array antenna without CPW. However, the increase of the gain becomes less steep at slot eight due to the decrease of the surface wave reached. This property agrees with the antenna pattern shown in Fig. 5.

In the case of the two-dimensional slot-array antenna fed by CPW, the coupling of the surface wave (TE wave) and the arrayed slots improves the H-plane antenna pattern, as shown in Fig. 6, and the power gain becomes higher than the two other antennas. The 8 × 3 slot-array antenna improved a power gain by 11 dB over the single-slot antenna at 94 GHz and has the power gain of 13 dBi for 94-GHz irradiation. However, the experimental data for 8 × 3 array antenna showed only a slight increase over the 4×3 array antenna. This means that the 8×3 array is not significantly more effective than the 4×3 array as long as the transmission efficiency is $0.83/\lambda_m$, and that additional improvement of the CPW is necessary to raise the transmission efficiency.

In Fig. 8, the data of the power gain when the signal was irradiated from the air side are also shown by small symbols and narrow lines. The figure shows that the gains when the signal was irradiated from the air side are smaller by 6 dB than those when the signal was irradiated through the substrate.

VI. CONCLUSIONS

The receiving properties of the slot-array antenna with parasitic slots, slot-array antenna fed by CPW, and two-dimensional slot-array antenna fed by CPW were compared and discussed at 94 GHz, both theoretically and experimentally. From these studies, we can conclude the following.

1) The power gain of the slot-array antenna with parasitic slots increased with the increase of the number of slots up to six slots. This improvement was caused by decreasing the surface-wave power in the substrate. However, the raise in the power gain with the increase of the number of slots from six to eight was insignificant.
2) In the case of the slot-array antenna fed by CPW, the power gain still increased with the increase of the number of slots from six to eight. This improvement was caused by sharpening the directivity perpendicular to the substrate. However, the H-plane pattern was almost the same compared to the slot-array antenna without CPW.
3) In the case of the two-dimensional slot-array antenna fed by CPW, the power gain was higher than the two other antennas. This improvement was caused by sharpening the directivity in the H-plane.

From these results, the fabricated 8×3 slot-array antenna had an improved power gain of 11 dB over the single-slot antenna at 94 GHz and a power gain of 13 dBi was obtained when the signal wave was irradiated from the dielectric side.

In the future, by improving the transmission efficiency of CPW, the power gain could be further increased.

REFERENCES

[1] R. S. Tahim, G. M. Hayashibara, and K. Chang, "Design and performance of W-band broad-band integrated circuit mixers," *IEEE Trans. Microwave Theory Tech.*, vol. MTT-31, pp. 277–283, Mar. 1983.

[2] T. Yoneyama, "Recent developed in NRD-guide technology," *Ann. Telecommun.*, vol. 47, nos. 11/12, pp. 17–23, 1992.

[3] K. Sakakibara, J. Hirokawa, M. Ando, and N. Goto, "Single-layer slotted waveguide arrays for millimeter wave applications," *IEICE Trans. Commun.*, vol. E79-B, no. 12, pp. 1765–1772, Dec. 1996.

[4] S. M. Wentworth, R. L. Rogers, J. G. Heston, D. P. Neikirk, and T. Itoh, "Millimeter wave twin slot antennas on layered substrates," *Int. J. Infrared Millim. Waves*, vol. 11, no. 2, pp. 111–131, Feb. 1990.

[5] S. S. Gearhart and G. M. Rebeiz, "A monolithic 250-GHz Schottky-diode receiver," *IEEE Trans. Microwave Theory Tech.*, vol. 42, pp. 2504–2511, Dec. 1994.

[6] M. C. Gaidis, H. G. LeDuc, M. Bin, D. Miller, J. A. Stern, and J. Zmuidzinas, "Characterization of low-noise quasi-optical SIS mixers for the submillimeter band," *IEEE Trans. Microwave Theory Tech.*, vol. 44, pp. 1130–1139, July 1996.

[7] D. F. Filipovic, W. Y. Ali-Ahmad, and G. M. Rebeiz, "Millimeter-wave double dipole antennas for high-gain integrated reflector illumination," *IEEE Trans. Microwave Theory Tech.*, vol. 40, pp. 962–967, May 1992.

[8] H. P. Moyer and R. A. York, "Active cavity-backed slot antenna using MESFET's," *IEEE Microwave Guided Wave Lett.*, vol. 3, pp. 95–97, Apr. 1993.

[9] B. K. Kormanyos, W. Harokopus, L. P. B. Katehi, and G. M. Rebeiz, "CPW-fed active slot antennas," *IEEE Trans. Microwave Theory Tech.*, vol. 42, pp. 541–545, Apr. 1994.

[10] H. Legay and L. Shafai, "A self-matching wide-band feed network for microstrip arrays," *IEEE Trans. Antennas Propagat.*, vol. 45, pp. 715–722, Apr. 1997.

[11] R. T. Gloutak, Jr., and N. G. Alexopoulos, "Two-arm eccentric spiral antenna," *IEEE Trans. Antennas Propagat.*, vol. 45, pp. 721–730, Apr. 1997.

[12] B. K. Kormanyos, P. H. Ostdiek, W. L. Bishop, T. W. Crowe, and G. M. Rebeiz, "A planar wide-band 80–200-GHz subharmonic receiver," *IEEE Trans. Microwave Theory Tech.*, vol. 41, pp. 1730–1737, Oct. 1993.

[13] T. Shimizu, Y. Abe, and Y. Yasuoka, "Thin-film slot antennas for 700GHz submillimeter wave radiation," *IEICE Trans. Electron.*, vol. E78-C, no. 8, pp. 1002–1006, Aug. 1995.

[14] T. Shimizu, Y. Abe, Y. Yasuoka, and K. Gamo, "Thin-film slot antennas for 2.5THz submillimeter radiation," *Jpn. J. Appl. Phys.*, vol. 35, no. 2B, pp. L266–L268, Feb. 1996.

[15] H. Kobayashi, M. Yuki, and Y. Yasuoka, "Effects of substrate thickness on the gain of millimeter and submillimeter wave slot antennas," *Trans. IEICE*, vol. 80-B-II, no. 1, pp. 54–62, Jan. 1997 (in Japanese).

[16] H. Kobayashi and Y. Yasuoka, "Design and fabrication of 94GHz slot array antennas," *Trans. IEICE*, vol. 79-B-II, no. 1, pp. 53–60, Jan. 1996 (in Japanese).

[17] Y. Yasuoka, H. Kobayashi, and T. Shimizu, "Antenna coupled thin-film far-infrared radiation detectors," in *Proc. SPIE IR Tech. Appl. XXII*, vol. 2744, Orlando, FL, Apr. 8–12, 1996, pp. 44–51.

[18] H. Kobayashi and Y. Yasuoka, "Receiving properties of slot array antennas with parasitic slots on dielectric substrates," *Trans. IEICE*, vol. 80-B-II, no. 10, pp. 862–870, Nov. 1997 (in Japanese).

[19] M. Kominami, D. M. Pozar, and D. H. Schaubert, "Dipole and slot elements and arrays on semi-infinite substrates," *IEEE Trans. Antennas Propagat.*, vol. AP-33, pp. 600–607, June 1985.

[20] T. Shimizu, H. Moritsu, and Y. Yasuoka, "Fabrication of the antenna coupled microbolometers," *Jpn. J. Appl. Phys.*, vol. 34, no. 12A, pt. 1, pp. 6352–6357, Dec. 1995.

[21] D. B. Rutledge, D. P. Neikirk, and D. P. Kasilingam, "Integrated circuit antennas," in *Infrared and Millimeter Waves*, K. J. Button, Ed. New York: Academic, 1983, vol. 10, pp. 34–45.

[22] J. D. Kraus, *Antennas*. New York: McGraw-Hill, 1950, pp. 57–126.

[23] C. A. Balanis, *Antenna Theory*. New York: Wiley, 1982, pp. 204–321.

Hiroaki Kobayashi received the B.S. degree in electrical engineering and the M.E. degree in electronic engineering from the National Defense Academy, Yokosuka, Japan, in 1987 and in 1992, respectively.

He is currently a Researcher at the National Defense Academy. He is engaged in research on infrared detectors, and millimeter- and submillimeter-wave antennas and detectors.

Mr. Kobayashi is a member of the Japan Society of Applied Physics and the Institute of Electronics, Information, and Communication Engineers (IEICE), Japan.

Yoshizumi Yasuoka graduated from the National Defense Academy, Yokosuka, Japan, in 1961. He received the M.E. and Ph.D. degrees in electrical engineering from Tohoku University, Sendai, Japan, in 1966 and 1969, respectively.

From 1969 to 1973, he was a Research Fellow at the Technical Research and Development Institute, Japan Defense Agency. In 1973, he joined the National Defense Academy, where he has been a Professor of electric engineering since 1980. From 1977 to 1978, he was a Visiting Scientist at the University of California at Berkeley. His research interests include millimeter- and submillimeter-wave detectors, mixers, and antennas, and high T_c superconducting mixers.

Dr. Yasuoka is a member of the Institute of Electrical Engineering of Japan, the Japan Society of Applied Physics, the Laser Society of Japan, the Japan Society of Infrared Science and Technology, and the Institute of Electronics, Information, and Communication Engineers (IEICE), Japan.